Desalination and Water Treatment
www.deswater.com

doi: 10.1080/19443994.2015.1100555

57 (2016) 19431–19442
September

Taylor & Francis
Taylor & Francis Group

Statistical modeling and optimization of the phosphorus biosorption by modified *Lemna minor* from aqueous solution using response surface methodology (RSM)

Dariush Naghipour[a], Kamran Taghavi[a], Jalil Jaafari[b], Yousef Mahdavi[c], Mohammad Ghanbari Ghozikali[d], Reza Ameri[e], Arsalan Jamshidi[f], Amir Hossein Mahvi[b,g,h,*]

[a]*School of Public Health, Guilan University of Medical Sciences, Rasht, Iran, Tel. +98 131 3229599; Fax: +98 131 3234155; emails: dr.naghipour@gmail.com (D. Naghipour), kam2000ir@yahoo.com (K. Taghavi)*
[b]*School of Public Health and Institute of Public Health Research, Tehran University of Medical Sciences, Tehran, Iran, Tel. +98 9352994768; email: Jalil.Jaafari@yahoo.com (J. Jaafari), Tel. +98 21 21 88 95 49 14; Fax: +98 21 2166 46 22 67; email: ahmahvi@yahoo.com (A. Hossein Mahvi)*
[c]*Faculty of Health, Department of Environmental Health Engineering, Health Sciences Research Center, Mazandaran University of Medical Sciences, Sari, Iran, Tel. +98 21 88 96 82 58; Fax: +98 21 66 46 22 67; email: mahdaviyusef@yahoo.com*
[d]*Tabriz Health Services Management Research Center, Department of Environmental Health Engineering, East Azerbaijan Province Health Center, Tabriz University of Medical Sciences, Tabriz, Iran, Tel. +98 4112333933; Fax: +9821 2166 46 22 67; email: ghanbary.mo@gmail.com*
[e]*Department of Environmental Engineering, Islamic Azad University, Science and Research Branch, Tehran, Iran, Tel. +98 21 88 96 82 58; Fax: +98 21 66 46 22 67*
[f]*Department of Environmental Health Engineering, School of Public Health, Yasuj University of Medical Sciences, Yasuj, Iran, Tel. +98 21 21 88 95 49 14; email: jamshidiarsalan@yahoo.com*
[g]*Center for Solid Waste Research, Institute for Environmental Research, Tehran University of Medical Sciences, Tehran, Iran*
[h]*National Institute of Health Research, Tehran University of Medical Sciences, Tehran, Iran*

Received 4 March 2015; Accepted 18 September 2015

ABSTRACT

Response surface methodology involving Box–Behnken design was used to evaluate the effects of three operating variables: pH, initial concentration of phosphorus, and adsorbent dosage on biosorption of phosphorus by modified *Lemna minor* by lab-scale batch study. Analysis of variance (ANOVA) showed pH, initial phosphorus concentration, interaction of phosphorus and adsorbent dose and the second-order effect of pH have values of "Prob. > F" less than 0.0500 indicating that model terms are significant for the biosorption of phosphorus. Optimum operational conditions for maximizing phosphorus biosorption were achieved at pH 4.8, initial phosphorus concentration of 19 mg/L and adsorbent dosage of 5.15 g/L. Under optimal value of parameters, high biosorption (89.2%) was obtained for phosphorus. Langmuir with 0.99 consistencies fitted better than Temkin, or Freundlich models. The maximum adsorption capacity of phosphorus was determined as 3.6 mg/g. Pseudo-second-order kinetic model exhibited the highest correlation with data. Results suggest that the modified *L. minor* has potential for biosorption as a low-cost and effective absorbent for phosphorus removal from aqueous solution.

*Corresponding author.

1944-3994/1944-3986 © 2015 Balaban Desalination Publications. All rights reserved.

Keywords: Response surface methodology; Phosphorus; *Lemna minor*; Biosorption

1. Introduction

Phosphorus compounds are commonly used in various consumer products and industries such as: fertilizers, water softening, detergents, metallurgy, paints, food, beverages, and pharmaceuticals [1]. Phosphorus concentration in municipal wastewater in the range of 4–15 mg/L can be considered as one of the main sources of phosphorus release into water bodies [2,3]. The presence of excess phosphorus compounds in aquatic systems causes rapid growth of phytoplankton and eutrophication in water bodies of rivers, lakes, and seas [4]. Removal of phosphorus compounds from effluents is compulsory in regions where the regulations of discharge standards are strict [5,6]. Therefore, it is necessary to find suitable treatment processes to remove phosphorus compounds from effluents. Different methods such as chemical precipitation [7,8], membrane technologies [9], biological processes [10,11], ion exchange [12], enzymatic treatment [13,14], rice husk [15,16], and adsorption [17] are being used for phosphorus removal from aqueous solutions. Each of these methods has specific advantages and disadvantages. Among these available alternatives, adsorption process is one of the effective methods that have been effectively used for many pollutant removals from aqueous solutions. Recently, different types of adsorbents have been employed for phosphorus removal, such as pumice [18], nano-particle resin Lewatit (FO36) [19], aluminum oxides [20], iron oxides [21], Ulmus leaves [22], fly ash [23], red mud [24], silicates [25], active carbon [26], niobium oxide [27], etc. However, many of these adsorbents have good efficiencies for adsorption, but some of them are expensive and with high maintenance cost. To optimize the adsorption processes, it is essential to develop novel alternative adsorbents with high adsorptive capacity. Consequently, it is urgent to find new adsorbents or biomaterials for adsorption of pollutants from aqueous solutions [15,28,29]. So, biosorption can be a feasible and useful alternative method to remove pollutants, being low cost, nonhazardous, with high adsorptive capacity, improved selectivity for specific pollutants, and being environment friendly [14,22,30,31]. The adsorptive capacity of an adsorbent can be increased by several modification methods [32–34]. Therefore, the natural medium's adsorption properties of the adsorbent can be improved by chemical pretreatments [34]. Aquatic plants play a key role as biosorbents for the removal of pollutants from aqueous solutions [35–37]. *Lemna minor* known as duckweed, is a free-floating aquatic plant that is widely distributed in many countries. *L. minor* is tolerant to cold weather and can survive in the temperature range of 35–95˚F. It is rapid growing and under optimum circumstances, it can be doubled in a week and adapt to a variety of conditions [38]. Previous studies have reported that *L. minor* has the potential for biosorption of contaminants such as nickel, cadmium, copper, fluoride, cadmium, methyl parathion, methyl and ethyl mercury, and dyes from aqueous solutions [39–42]. Until now no report on the application of *L. minor* to phosphorus removal has been found.

The present study aims to investigate the biosorption of phosphorus by modified *L. minor* as biosorbent. The effects of various parameters such as pH of solution, initial phosphorus concentration, and adsorbent dosage were examined. The Box–Behnken experimental design model was used for precisely on finding the role of individual process parameters and for the optimization of parameters. The Langmuir, Freundlich and Temkin models were used to describe equilibrium isotherms. Also various kinetic models were tested to describe the sorption data.

2. Materials and methods

2.1. Preparation of biomass

L. minor was collected from Babol, Iran. Before use, biomass was washed several times using sterile distilled water and dried under sunlight for 3 d. To prepare the modified biomass, *L. minor* was immersed in 0.1 M HCl for 5 h. Finally, modified *L. minor* was washed with distilled water several times and dried [43]. After drying, all the adsorbents were straitened to obtain particle size of 2 mm to use for adsorption studies.

2.2. Adsorption experiments

All experiments were conducted in batch system using a 250 mL reactor containing 100 ml of experimental solution, at 25˚C. Seventeen biosorption experiments designed by response surface methodology (RSM) were performed at the equilibrium time of 40 min, to investigate the influence of solution pH, initial phosphorus concentration, and the dosage of modified *L. minor* on phosphorus removal. A phosphorus stock solution (100 mg/L) was prepared by dissolving KH_2PO_4 salt (analytical reagent grade) in double-distilled water. The experimental solution was prepared by diluting the stock solution to desired concentration using distilled water. Samples with different modified *L. minor* contents were agitated on the shaker at 200 rpm. The pH values of solutions were adjusted with 1 M HCl and 1 M NaOH solutions. All reagents were of analytical grade. Distilled water was used through all the experiments. Samples were separated through 0.45-μm filters at the end of agitation period. The residual phosphate concentrations were determined using the method of the reduction of Molybdophosphate and detected at a wavelength of 470 nm by a Vis spectrophotometer (Shimadzo-1700, Japan). Phosphorus biosorption by modified *L. minor* was determined as according Eq. (1):

$$Q_E = (C_0 - C_t) \times \frac{100}{C_0} \tag{1}$$

where Q_E is the percentage of phosphorus adsorbed by biomass, C_0 is the initial concentration of phosphorus in mg/L and C_t is the final concentration of phosphorus in mg/L.

2.3. Response surface methodology

RSM is an approach that joins mathematical and statistical tools and techniques, and is valuable for developing, improving, and optimizing the processes [44] and could evaluate the relative significance of several affecting factors even in the presence of complex interactions. Other advantage of the RSM is the reduction in number of experiments when there are several factors incorporated in the study. The present study, aims to investigate the effect of independent variables on the response functions and investigate the optimum condition for the biosorption of phosphorus by modified *L. minor*. Box–Behnken design (BBD) and RSM from *R* statistic software, package of RSM 2.6 were used for designing and optimizing variables [45]. BBD of three independent variables with three levels for any variable as low (−1), medium (0), and high (+1) was used to find the optimum pH, biosorbent dose, and initial phosphorus concentration. This practice makes designs with desirable statistical properties, but, most importantly, with only a fraction of the trials required for a 3-level factorial. Since there are only three levels, the quadratic model is suitable. The number of experiments required for BBD can be calculated as follows:

$$N = k^2 + k + cp \tag{2}$$

where N is the total number of experiments, k is the number of variables and cp is the replicate number of the central point. Therefore, in this study, 17 runs for a three-parameter experimental design were required by BBD. In the BBD model, pH of (3–7), initial phosphorus concentration of (10–20 mg/L), and adsorbent concentration of (2–6 g/L) were taken as input variables. In the RSM, each response Y can be represented by a mathematical equation to correlate the dependent and independent variables. For better accuracy, the second-order polynomial regression model equation was widely used to fit the experimental data and simultaneously to solve multivariate equations, to optimize the processes and the products [15,46,47]. The second-order polynomial regression model equation is expressed as:

$$Y_i = \beta_0 + \sum \beta_i x_i + \sum \beta_{ii} x_i^2 + \sum \beta_{ij} x_i x_j + \varepsilon \tag{3}$$

where Y is the predicted response associated with each factor level combination, β_0 is the intercept term, β_i is the slope or linear effect of the input factor x_i, β_{ii} is the quadratic effect, β_{ij} is the linear interaction effect between input factors, and ε is the residual term.

3. Results and discussion

3.1. Model fitting and statistical analysis

For statistical calculations, each factor was coded at three levels according to the following equation:

$$x_i = \frac{X_i - X_0}{\Delta X} \tag{4}$$

where x_i is the code for the real values (X_i); X_0 is the value of X_i at the center point, and ΔX represents the step change. Table 1 displays the coded and uncoded levels of these independent variables. The response surface regression results from BBD are shown in Table 2.

By using multiple regression analysis on the experimental result, the quadratic polynomial model for the predicted biosorption of phosphorus basis coded values was shown as below:

$$Y = 87.96 - 2.95X_1 + 3.50X_2 + 0.89X_3 - 20.11X_1^2 - 2.92X_2^2 - 2.21X_3^2 + 0.66X_1X_2 + 0.21X_1X_3 + 2.1X_2X_3 \tag{5}$$

Table 1
Experimental factors in coded units and experimental responses

S. no.	Variable	Name	Variable level		
			−1	0	+1
1	X_1	pH	3	5	7
2	X_2	Initial phosphorus concentration (mg/L)	10	15	20
3	X_3	Adsorbent concentration (g/L)	2	4	6

Table 2
Experimental design matrix and results

Run no.	Std. order	Coded variable			Actual variable			Response		
		x_1	x_2	x_3	x_1	x_2	x_3	Experimental	Predicted	Residual
1	8	1	0	1	7	15	6	63.86	87.74	−0.35
2	3	−1	1	0	3	20	4	73.4	68.38	−0.79
3	7	−1	0	1	3	15	6	67.6	78.8	1.912
4	5	−1	0	−1	3	15	2	67.85	61.05	−1.911
5	13	0	0	0	5	15	4	88.11	87.74	0.37
6	11	0	−1	1	5	10	6	80.71	87.74	−0.62
7	4	1	1	0	7	20	4	67.1	87.74	0.559
8	6	1	0	−1	7	15	2	63.25	83.74	0.824
9	9	0	−1	−1	5	10	2	81.54	82.62	−1.89
10	16	0	0	0	5	15	4	87.02	62.16	−0.294
11	17	0	0	0	5	15	4	89.21	89.12	−0.794
12	1	−1	−1	0	3	10	4	64.1	87.74	0.055
13	15	0	0	0	5	15	4	89.1	62.44	0.812
14	10	0	1	−1	5	20	2	80.73	66.54	0.312
15	12	0	1	1	5	20	6	88.32	65.65	1.454
16	2	1	−1	0	7	10	4	55.13	66.21	−2.049
17	14	0	0	0	5	15	4	86.4	70.81	2.675

The validity of the models was tested with analysis of variance (ANOVA) of regression variables of the predicted response surface quadratic model and presented in Tables 3 and 4. The statistical significance of all the terms of the model was tested by the *F*-value and the *p*-value. The *F*-value is used as the check for comparing the curvature variance with residual variance. *F*-value from the model implied the significance of the model similarity, and the value of probability $> F$ less than 0.05 indicated that the model terms are significant. Table 4 shows ANOVA for the response surface quadratic model. The *F*-value (108.11) with a low probability $> F$ (<0.0001) indicates that model terms are significant for the regression model. The values of *R*-squared (R^2) and adjusted *R*-squared (Adj. R^2) were 0.978 and 0.951, respectively, which indicates a high correlation between the observed and the predicted values. It could be seen from Table 3, that the first-order effects of pH (X_1) and initial phosphorus concentration (X_2) are highly significant compared to the first-order effect of adsorbent concentration (X_3). Even the

Table 3
ANOVA results for the response surface quadratic model for phosphorus biosorption

Source of variations	Degrees of freedom	Sum of squares	Mean square	*F*-value	Prob. (>*F*)
Regression	9	2,015.8	671.94	108.11	<0.0001
Residual	7	43.53	6.21		
Total	16	2,059.33			
Lack of fit	3	37.3	8.08	8.01	0.036
Pure error	4	6.2	1.55		

Table 4
Estimated regression coefficient and corresponding t and p-value

Model term	Coefficient estimate	Standard error	t-value	p-value
Intercept	87.96	1.11	78.90	<0.0001
X_1	−2.95	0.88	−3.34	0.012
X_2	3.50	0.88	3.98	0.005
X_3	0.89	0.88	1.00	0.34
X_1X_2	0.66	1.24	0.535	0.60
X_1X_3	0.21	1.24	0.17	0.86
X_2X_3	2.10	1.24	1.68	0.035
X_1^2	−20.11	1.21	−16.55	<0.0001
X_2^2	−2.92	1.21	−2.40	0.046
X_3^2	−2.21	1.21	−1.82	0.11

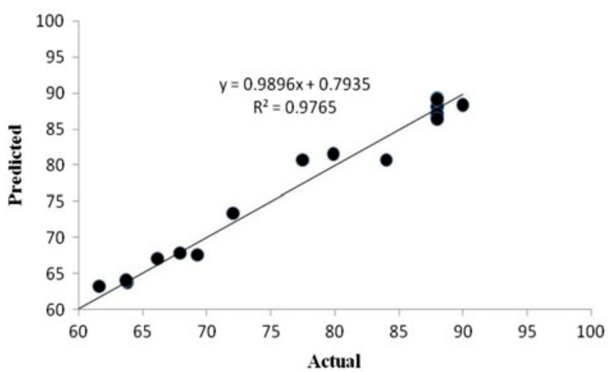

Fig. 1. Comparison of experimental (%) vs. predicted (%) data by RSM.

first-order effect of adsorbent concentration (X_3) was not the significant term.

An interaction term coefficient of phosphorus concentration and adsorbent concentration (X_2X_3) was statistically significant due to very small p-values ($p < 0.05$) which indicate that these terms were important to the biosorption of phosphorus. The second-order effect of pH (X_1^2) was much significant compared to phosphorus concentration (X_2^2) and adsorbent concentration (X_3^2) as suggested by the model. The p-values in the second-order effect of adsorbent concentration (X_3^2) was not significant ($p > 0.05$). Optimum operating parameters were found to maximize the biosorption of phosphorus from quadratic model equations. Optimum operating parameters of medium pH, initial phosphorus concentration, and adsorbent concentrations were 4.8, 19 (mg/L), and 5.15 (g/L), respectively. The biosorption of phosphorus efficiency under the evaluated optimum experimental conditions was 89.2%, which was in good agreement with the predicted value of 90.2%, suggesting that the model was reliable in this study (Fig. 1).

3.2. Response surface plots

In order to explain the interaction effect of variables in the phosphorus biosorption, the three-dimensional (3D) plots for the predicted responses were illustrated.

The effect of initial phosphorus concentration and pH in agitation time of 40 min on the biosorption of phosphorus by modified *L. minor* is shown in Fig. 2(a). It shows that biosorption efficiency increases with increasing phosphorus concentration up to 10–20 mg/L.

Maximum percentage biosorption of phosphorus >80% was acquired at pH 5 and high initial phosphorus concentration (20 mg/L), as observed by several workers [24,48]. This phenomenon is mainly attributed to an increase in the adsorbable surface area and the accessibility of further adsorption sites. The adsorption of phosphorus most likely occurs via surface exchange reaction until the surface efficient sites are completely occupied. Subsequently, the phosphorus molecules diffuse into the pores of the modified *L. minor* for promoting reactions. As shown in Fig. 2(a), biosorption efficiency is found to decrease when moving away from these points, since either increase or reduction in the pH value results in turn down of the biosorption efficiency.

Thermodynamic studies revealed that depending on the aqueous solution pH, various forms of phosphorus can be predominant, such as H_3PO_4, $H_2Po_4^-$, HPo_4^{2-} and Po_4^{3-}. As shown in Fig. 2(a) and (b), at initial pH values 3.0–5.0, the biosorption of phosphorus increased, whereas above 5.0, the biosorption efficiency decreased. At a low initial pH in the solution, protons can compete with H_3PO_4 for the active sites in the surface of modified L. minor, that is predominant in pH of 3, resulting active sites in adsorbents surface decrease at a low pH, so the biosorption capacity of phosphate decrease. On the other hand, in the higher

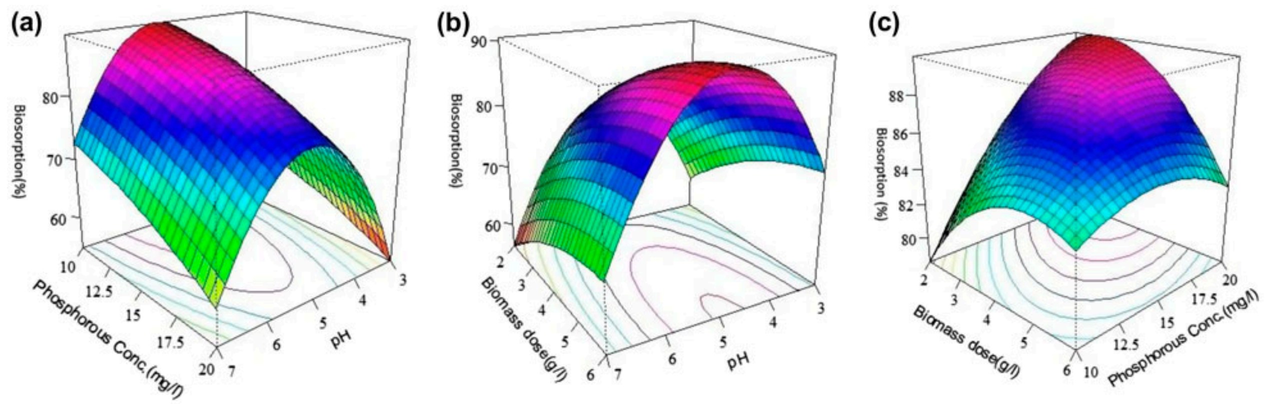

Fig. 2. 3D response surface plot. Interaction plot of (a) phosphorus concentration and pH, (b) biomass dose and pH, and (c) phosphorus concentration and biomass dose, on phosphorus biosorption efficiency.

pH due to high concentration of hydroxide groups, which competed strongly with phosphate for binding to the active sites, biosorption efficiency decreased. Also, the main phosphate group at pH > 7 is $H_2Po_4^-$, which have a higher appeal for the biosorption in modified *L. minor* [49]. Therefore, the nature of the phosphorus species is the key factor in the high-phosphorus biosorption efficiency at lower pH.

Fig. 2(b) reveals the interaction effect between pH and biomass dose has similar trend as observed for biomass dose. At pH 5, increasing biomass dose had a slight negative effect on biosorption of phosphorus, but at lower and higher pH values the trend of biosorption was decreased. The maximum value of biosorption determined was >80% at pH 5 and 6 g/L of modified *L. minor*. Fig. 2(c) represents the surface plot indicating effects of biomass dose and initial phosphorus concentrations on phosphorus biosorption. In similar studies, maximum adsorption of phosphorus for red mud and pumice in pH ranging from 5 to 7, and 6.5 for activated alum were achieved [18,24,50]. It shows that biosorption increases with increasing phosphorus concentration up to 10–15 mg/L and afterward shows a slight decrease in low dose of adsorbent. A similar trend was also observed in low dose of adsorbent. At higher concentration with increasing phosphorus concentration and adsorbent dose, maximum phosphorus biosorption was achieved.

3.3. Biosorption isotherms

In order to estimate the maximum biosorption capacity, numerous sorption isotherm models were used to explain the adsorption process. Among all the available models, Langmuir 1 and 2, Freundlich and Temkin adsorption isotherms were tested for equilibrium description at ambient temperature. To study the equilibrium adsorption isotherm, experiments were performed with adsorbent dosage of 4 g/L and initial phosphorus concentrations of 10–20 mg/L for 120 min contact time at pH 5, temperature of 25˚C, and 200 rpm. Table 5 shows the equations and parameters obtained for the different investigated isotherm models. Where in Langmuir model, q_e is the amount of phosphorus adsorbed by modified *L. minor* at equilibrium concentration of phosphorus (C_e), q_m and b are the Langmuir constants representing adsorption capacity and Langmuir constant energy of adsorption, respectively. In Freundlich isotherm, K_F and n are the Freundlich constants representing the adsorption capacity and adsorption intensity that informs about the heterogeneity characteristic of the surface sites, respectively. In Temkin isotherm, K_t is the Temkin isotherm equilibrium binding constant (L/g) and B_1 is a constant related to heat of sorption (J/mg). Fig. 3 shows a plot of the isotherm models for the biosorption of phosphorus onto modified *L. minor*. According to the coefficients in Table 5, the R^2 values obtained for the Freundlich, Langmuir 1 and 2, and Temkin isotherm models were 0.96, 0.991, 0.88, and 0.98, respectively. Thus, biosorption of phosphorus nicely fitted with the Langmuir 1 isotherm model. These results comply with other studies on phosphorus adsorption by modified pumice [50], modified activated alumina [51], modified and nanozeolite *Y* [52]. Also, the maximum biosorption capacity (q_m) was obtained as 2.02 mg/g for modified *L. minor*. In similar studies, The biosorption capacity (q_m) for other adsorbent's for phosphorus adsorption were 0.58 mg/g for red mud [53], 1.6 mg/g for FO_36 [19] and 16.6 mg/g for hydrous niobium oxide [27].

Further, a dimensionless constant can be expressed in terms of a dimensionless constant separation factor

Table 5
Characteristics and isotherm constants for phosphorus biosorption by modified *L. minor*

Isotherm model	Principle equation	Linear equation	Parameters	
Freundlich	$q_e = K_F C_e^{\frac{1}{n}}$	$\log(q_e) = \log K_F + \frac{1}{n \log C_e}$	R^2	0.96
			K_F ($mg^{1-(1/n)}$ $L^{1/n}$ g–1)	3.96
			n	3.37
Langmuir 1	$q_e = \frac{q_m b C_e}{1 + bC_e}$	$\frac{C_e}{q_e} = \frac{C_e}{q_m} + \frac{1}{q_m b}$	R^2	0.991
			q_m (mg/g)	2.02
			b (L/mg)	1.3
			R_L	0.048
Langmuir 2		$\frac{1}{q_e} = \frac{1}{q_m b C_e} + \frac{1}{q_m}$	R^2	0.87
			q_m	2.13
			b (L/mg)	1.56
			R_L	0.040
Temkin	$q_e = \frac{RT}{b_1} \ln(k_t C_e)$	$q_e = B_1 \ln(k_t) + B_1 \ln(C_e)$	R^2	0.98
			b_1 (J/mol)	245
			K_T (L/mg)	99

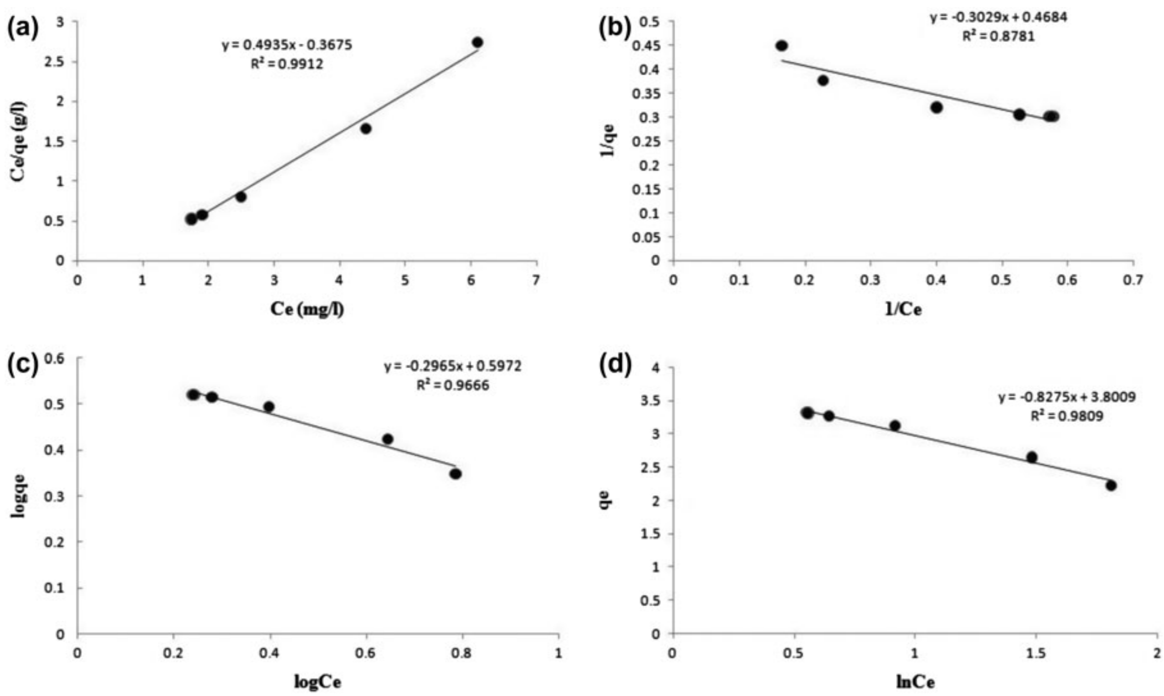

Fig. 3. Langmuir 1 (a) and 2 (b), Freundlich (c) and Temkin (d) plot for phosphorus biosorption onto modified *L. minor*.

(R_L), also calculated to test the favorability of adsorption by the following relationship:

$$R_L = \frac{l}{l + bC_0} \tag{6}$$

where C_0 is the initial phosphorus concentration (mg/L) and b is the Langmuir isotherm constant. The value of separation parameter R_L presents important information about the nature of adsorption. The value of R_L signified the type of Langmuir isotherm to be irreversible ($R_L = 0$), favorable ($0 < R_L < 1$), linear ($R_L = 1$) or unfavorable [54,55]. The values of the separation factor R_L are between 0 and 1 indicating favorable adsorption of phosphorus onto modified *L. minor* (Table 5).

3.4. Kinetic analysis

In order to investigate the biosorption mechanism of phosphorus onto modified *L. minor* and rate controlling steps that include mass transport and chemical reaction processes, a kinetic modeling was tested; pseudo-first- and pseudo-second-order kinetic models have been used for testing experimental data. Adsorption kinetic experiments were fitted with linearized forms of pseudo-first order (Eq. (7)) and pseudo-second order (Eq. (8)) by 15 mg/L initial phosphorus concentration with modified *L. minor* dosage of 5 g/l at pH 5 for different contact times 0–120 min and shaking speed of 200 rpm.

$$\log(q_e - q_t) = \log q_e - \frac{k_1}{2.303}t \tag{7}$$

$$\frac{t}{q_t} = \frac{1}{k_2 q_e^2} + \frac{1}{q_e}t \tag{8}$$

where q_e and q_t are the adsorption amount (mg/g) at equilibrium and any time t, respectively, k_1 (g/mg/min) the rate constant in the pseudo-first-order adsorption process and k_2 (g/mg/min) the rate constant for the pseudo-second-order adsorption reaction. The adsorption rate constant (k_1) for phosphorus biosorption was determined experimentally by plotting log ($q_e - q_t$) vs. t that is shown in Fig. 4(a). In the latter case, kinetic data were plotted between t/q_t and t (Fig. 4(b)). It is evident from the plots that the correlation coefficient (R^2) obtained from the figure was close to 1.0, showing that the phosphorus biosorption processes by modified *L. minor* is an excellent fit with the pseudo-second-order model. The kinetic rate constants such as: the k_2, regression cefficients, R^2, the experimental ($q_{eq,exp}$) and calculated ($q_{eq,cal}$) equilibrium uptake values obtained from second-order kinetic model are given in Table 6.The calculated value of q_e was 3.43 mg/g, agreeing with the experimental value 3.6 mg/g. This result further confirmed that the adsorption process of phosphorus by modified *L. minor* followed a pseudo-second-order reaction mechanism, and the adsorption rate was mainly controlled by the chemical bonding or chemisorptions. Similar results were also found in some other adsorptions of phosphorus by pumice [18], red mud [53], $ZnCl_2$-activated coir pith carbon [56], and calcined alunite [57].

3.5. Characterization

The scanning electron microscopy (SEM) image of the modified *L. minor* before and after biosorption of

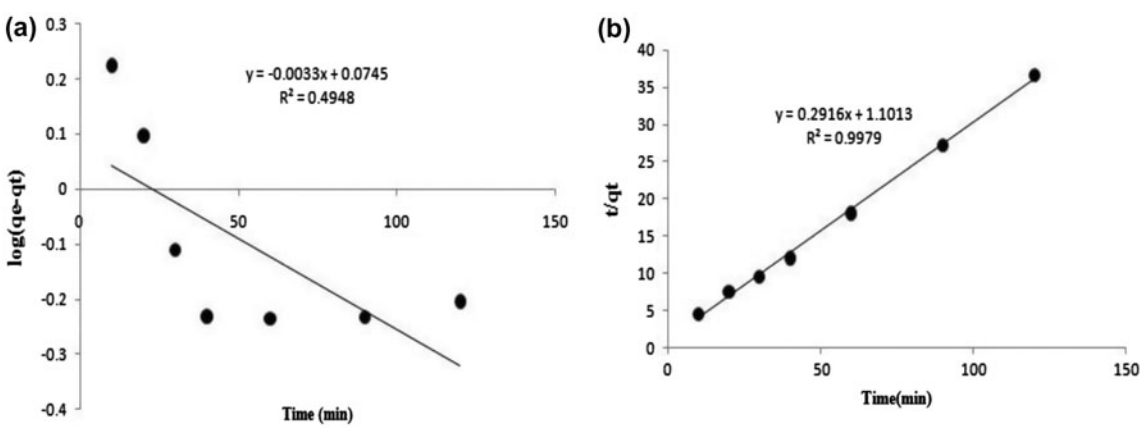

Fig. 4. Adsorption kinetic plots for biosorption of phosphorus on modified *L. minor*: (a) pseudo-first-order kinetics and (b) pseudo-second-order kinetics.

Table 6
Kinetic parameters obtained from pseudo-second-order model for biosorption of phosphorus by modified *L. minor*

		Second-order model		
Initial phosphorus conc. (mg/L)	$q_{e,exp}$ (mg/g)	K_2	$q_{e,cal}$ (mg/g)	R^2
15	3.6	0.077	3.43	0.997

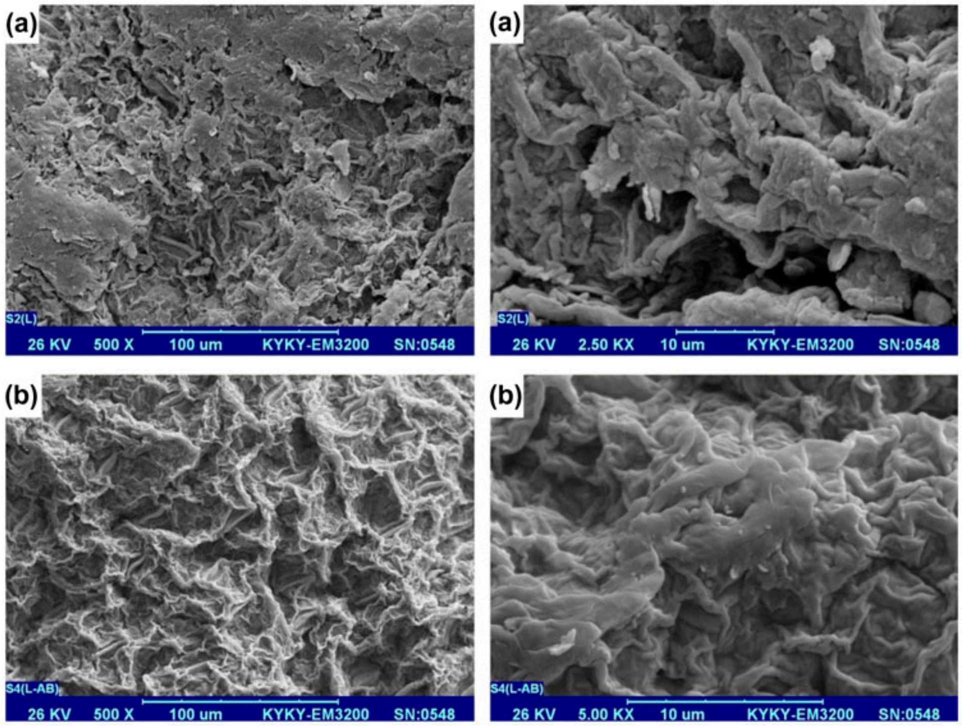

Fig. 5. Morphological (SEM image) details of modified *L. minor* before (a) and after (b) phosphorus biosorption.

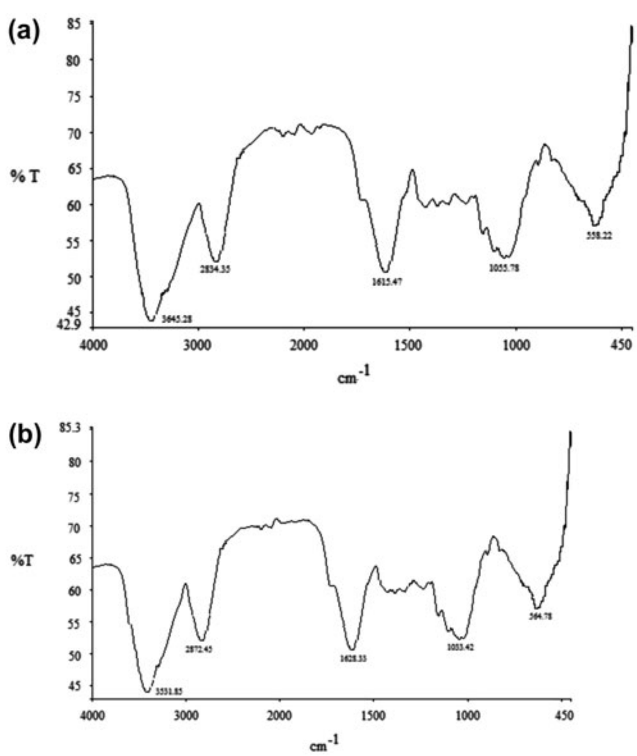

Fig. 6. FTIR spectra of modified *L. minor* before (a) and after (b) phosphorus biosorption.

phosphorus is shown in Fig. 5. The SEM images indicated good organization and uniform porosity, large and a series of irregular cavitations distributed around the surface on the sample surface of modified *L. minor* that provides large surface area for adsorption. However, no significant changes occurred in morphology of the adsorbent surface after phosphorus biosorption. For further characterization, the FTIR of the modified *L. minor* before and after the biosorption of the phosphorus are shown in Fig. 6(a) and (b), respectively. The characteristic peaks at around 1,615 and 1,055 cm^{-1} assigned to the amino and hydroxyl groups, respectively, both shifted to 1,628 and 1,033 cm^{-1} wave number, respectively and the intensities of the two peaks became stronger. The presence of absorption bands at 3,645 and at 2,834 cm^{-1} are due to the presence of H-bridges [58].

4. Conclusion

In this study, the biosorption of phosphorus on modified *L. minor* have been carried out. The RSM involving BBD and regression of analysis is used in finding the effect of the input variables (pH, biosorbent dosage, phosphorus concentration) with the percentage of phosphorus biosorption.

The second-order polynomial equation model whose validity is agreed upon is estimated using

ANOVA statistical testing, found pH, initial phosphorus concentration, interaction of phosphorus, and adsorbent concentration and the second-order effect of pH was found to have a significant effect on the biosorption of phosphorus. The optimum biosorption conditions were determined as initial pH 4.8, initial phosphorus concentration 19.3 mg/L, biosorbent concentration 5.15 g/L. Maximum biosoption of phosphorus was observed to be 89.2% under optimum experimental conditions. The results indicate that modified *L. minor* is an effective biosorbent for phosphorus removal. The results of equilibrium adsorption were fitted to different isotherm equations. The Langmuir isotherm model is in good agreement with the equilibrium data since it presents higher R^2 values than others. Different kinetic models were also tested, and the pseudo-second-order model was found to be the applicable kinetic model in the present study.

Acknowledgments

This research has been supported by Tehran University of Medical Sciences & Health Services under Grant No. 94-03-61-30003.

References

[1] A.H. Mahvi, S.J.A.-D. Ebrahimi, A. Mesdaghinia, H. Gharibi, M.H. Sowlat, Performance evaluation of a continuous bipolar electrocoagulation/electrooxidation–electroflotation (ECEO–EF) reactor designed for simultaneous removal of ammonia and phosphate from wastewater effluent, J. Hazard. Mater. 192 (2011) 1267–1274.

[2] J. Jaafari, A. Mesdaghinia, R. Nabizadeh, M. Hoseini, H. kamani, A.H. Mahvi, Influence of upflow velocity on performance and biofilm characteristics of Anaerobic Fluidized Bed Reactor (AFBR) in treating high-strength wastewater, J. Environ. Health Sci. Eng. 12 (2014) 139.

[3] Y. Esfandyari, Y. Mahdavi, M. Seyedsalehi, M. Hoseini, G.H. Safari, M.G. Ghozikali, H. Kamani, J. Jaafari, Degradation and biodegradability improvement of the olive mill wastewater by peroxi-electrocoagulation/electrooxidation-electroflotation process with bipolar aluminum electrodes, Environ. Sci. Pollut. Res. 22 (2014) 6288–6297.

[4] S.-X. Li, L.-H. Chen, F.-Y. Zheng, X.-G. Huang, Influence of eutrophication on metal bioaccumulation and oral bioavailability in oysters, *Crassostrea angulata*, J. Agric. Food Chem. 62 (2014) 7050–7056.

[5] O. Oenema, L. van Liere, O. Schoumans, Effects of lowering nitrogen and phosphorus surpluses in agriculture on the quality of groundwater and surface water in the Netherlands, J. Hydrol. 304 (2005) 289–301.

[6] J. Jafari, A. Mesdaghinia, R. Nabizadeh, M. Farrokhi, A.H. Mahvi, Investigation of anaerobic fluidized bed reactor/aerobic mov-ing bed bio reactor (AFBR/MMBR) system for treatment of currant wastewater, Iran. J. Public Health 42 (2013) 860–867.

[7] T. Clark, T. Stephenson, P. Pearce, Phosphorus removal by chemical precipitation in a biological aerated filter, Water Res. 31 (1997) 2557–2563.

[8] F. Gholami-Borujeni, A.H. Mahvi, S. Naseri, M.A. Faramarzi, R. Nabizadeh, M. Alimohammadi, Application of immobilized horseradish peroxidase for removal and detoxification of azo dye from aqueous solution, Res. J. Chem. Environ. 15 (2011) 217–222.

[9] Z. Geng, E. Hall, P. Berube, Membrane fouling mechanisms of a membrane enhanced biological phosphorus removal process, J. Membr. Sci. 296 (2007) 93–101.

[10] S. Tsuneda, T. Ohno, K. Soejima, A. Hirata, Simultaneous nitrogen and phosphorus removal using denitrifying phosphate-accumulating organisms in a sequencing batch reactor, Biochem. Eng. J. 27 (2006) 191–196.

[11] A. Mahvi, R. Nabizadeh, M. Pishrafti, Evaluation of single stage USBF in removal of nitrogen and phosphorus from wastewater, Eur. J. Sci. Res. 23 (2008) 204–211.

[12] L.M. Blaney, S. Cinar, A.K. Sengupta, Hybrid anion exchanger for trace phosphate removal from water and wastewater, Water Res. 41 (2007) 1603–1613.

[13] F. Gholami-Borujeni, A.H. Mahvi, S. Nasseri, M.A. Faramarzi, R. Nabizadeh, M. Alimohammadi, Enzymatic treatment and detoxification of acid orange 7 from textile wastewater, Appl. Biochem. Biotechnol. 165 (2011) 1274–1284.

[14] S.D. Ashrafi, S. Rezaei, H. Forootanfar, A.H. Mahvi, M.A. Faramarzi, The enzymatic decolorization and detoxification of synthetic dyes by the laccase from a soil-isolated ascomycete, *Paraconiothyrium variabile*, Int. Biodeterior. Biodegrad. 85 (2013) 173–181.

[15] S. Ashrafi, H. Kamani, J. jaafari, A. Mahvi, Experimental design and response-surface modeling for optimization of fluoroquinolone removal from aqueous solution by NaOH-modified rice husk Desalin. Water Treat. (2015) 1–9.

[16] S. Ashrafi, H. Kamani, H. Soheil Arezomand, N. Yousefi, A. Mahvi, Optimization and modeling of process variables for adsorption of Basic Blue 41 on NaOH-modified rice husk using response surface methodology, Desalin. Water Treat. (2015) 1–9.

[17] S. Tian, P. Jiang, P. Ning, Y. Su, Enhanced adsorption removal of phosphate from water by mixed lanthanum/aluminum pillared montmorillonite, Chem. Eng. J. 151 (2009) 141–148.

[18] G.H. Safari, M. Zarrabi, M. Hoseini, H. Kamani, J. Jaafari, A.H. Mahvi, Trends of natural and acid-engineered pumice onto phosphorus ions in aquatic environment: Adsorbent preparation, characterization, and kinetic and equilibrium modeling, Desalin. Water Treat. (2014) 1–13.

[19] L. Rafati, R. Nabizadeh, A.H. Mahvi, M.H. Dehghani, Removal of phosphate from aqueous solutions by iron nano-particle resin Lewatit (FO36), Korean J. Chem. Eng. 29 (2012) 473–477.

[20] K. Karageorgiou, M. Paschalis, G.N. Anastassakis, Removal of phosphate species from solution by adsorption onto calcite used as natural adsorbent, J. Hazard. Mater. 139 (2007) 447–452.

[21] Z. Hongshao, R. Stanforth, Competitive adsorption of phosphate and arsenate on goethite, Environ. Sci. Technol. 35 (2001) 4753–4757.
[22] A. Mahvi, F. Gholami, S. Nazmara, Cadmium biosorption from wastewater by *Ulmus* leaves and their ash, Eur. J. Sci. Res. 23 (2008) 197–203.
[23] S. Lu, S. Bai, L. Zhu, H. Shan, Removal mechanism of phosphate from aqueous solution by fly ash, J. Hazard. Mater. 161 (2009) 95–101.
[24] C.-J. Liu, Y.-Z. Li, Z.-K. Luan, Z.-Y. Chen, Z.-G. ZHANG, Z.-P. Jia, Adsorption removal of phosphate from aqueous solution by active red mud, J. Environ. Sci. 19 (2007) 1166–1170.
[25] T. Kasama, Y. Watanabe, H. Yamada, T. Murakami, Sorption of phosphates on Al-pillared smectites and mica at acidic to neutral pH, Appl. Clay Sci. 25 (2004) 167–177.
[26] D. Bhargava, S. Sheldarkar, Use of TNSAC in phosphate adsorption studies and relationships. Literature, experimental methodology, justification and effects of process variables, Water Res. 27 (1993) 303–312.
[27] L.A. Rodrigues, M.L.C.P. da Silva, Thermodynamic and kinetic investigations of phosphate adsorption onto hydrous niobium oxide prepared by homogeneous solution method, Desalination 263 (2010) 29–35.
[28] S. Guendouz, N. Khellaf, M. Zerdaoui, M. Ouchefoun, Biosorption of synthetic dyes (Direct Red 89 and Reactive Green 12) as an ecological refining step in textile effluent treatment, Environ. Sci. Pollut. Res. 20 (2013) 3822–3829.
[29] V. Gupta, Application of low-cost adsorbents for dye removal—A review, J. Environ. Manage. 90 (2009) 2313–2342.
[30] A. Selatnia, M. Bakhti, A. Madani, L. Kertous, Y. Mansouri, Biosorption of Cd^{2+} from aqueous solution by a NaOH-treated bacterial dead *Streptomyces rimosus* biomass, Hydrometallurgy 75 (2004) 11–24.
[31] A. Mahvi, Application of agricultural fibers in pollution removal from aqueous solution, Int. J. Environ. Sci. Technol. 5 (2008) 275–285.
[32] A. John Peter, T. Viraraghavan, Removal of thallium from aqueous solutions by modified *Aspergillus niger* biomass, Bioresour. Technol. 99 (2008) 618–625.
[33] H. Yazıcı, M. Kılıç, M. Solak, Application of low-cost adsorbents for dye removal—A review, J. Hazard. Mater. 151 (2008) 669–675.
[34] A. Kapoor, T. Viraraghavan, Biosorption of heavy metals on Aspergillus niger: Effect of pretreatment, Bioresour. Technol. 63 (1998) 109–113.
[35] P. Wang, C. Wang, X.-R. Wang, J. Hou, S. Zhang, The effect of hydrodynamics on nitrogen accumulation and physiological characteristics of *Vallisneria spiraslis* L in eutrophicated water, Afr. J. Biotechnol. 7 (2008) 2424–2433.
[36] N. Khellaf, M. Zerdaoui, Phytoaccumulation of zinc by the aquatic plant, *Lemna gibba* L, Bioresour. Technol. 100 (2009) 6137–6140.
[37] S. Guendouz, N. Khellaf, H. Djelal, M. Ouchefoun, Simultaneous biosorption of the two synthetic dyes, Direct Red 89 and Reactive Green 12 using nonliving macrophyte *L. gibba* L, Desalin. Water Treat. (2014) 1–9.
[38] N.R. Axtell, S.P. Sternberg, K. Claussen, Lead and nickel removal using *Microspora* and *Lemna minor*, Bioresour. Technol. 89 (2003) 41–48.
[39] S. Saygideger, O. Gulnaz, E.S. Istifli, N. Yucel, Adsorption of Cd (II), Cu (II) and Ni (II) ions by *Lemna minor* L.: Effect of physicochemical environment, J. Hazard. Mater. 126 (2005) 96–104.
[40] L.B. Lim, N. Priyantha, C.M. Chan, D. Matassan, H.I. Chieng, M. Kooh, Adsorption behavior of methyl violet 2B using duckweed: Equilibrium and kinetics studies, Arabian J. Sci. Eng. 39 (2014) 1–9.
[41] M.A. Zazouli, D. Belarak, F. Karimnezhad, F. Khosravi, Removal of Fluoride from Aqueous Solution by Using of Adsorption onto Modified Lemna Minor: Adsorption Isotherm and Kinetics Study, J. Mazandaran Univ. Med. Sci. (JMUMS) 23 (2014) 195–204.
[42] S.-X. Li, Z. Feng-Ying, H. Yang, N. Jian-Cong, Thorough removal of inorganic and organic mercury from aqueous solutions by adsorption on *Lemna minor* powder, J. Hazard. Mater. 186 (2011) 423–429.
[43] T. Padmesh, K. Vijayaraghavan, G. Sekaran, M. Velan, Batch and column studies on biosorption of acid dyes on fresh water macro alga *Azolla filiculoides*, J. Hazard. Mater. 125 (2005) 121–129.
[44] N.U. Papila, Neural network and polynomial-based response surface techniques for supersonic turbine design optimization (Ph.D Thesis), University of Florida 2001.
[45] R.V. Lenth, Response-Surface Methods in R, using rsm, J. Stat. Software 32 (2009) 1–17.
[46] S. Ashrafi, S. Nasseri, M. Alimohammadi, A. Mahvi, M. Faramarzi, Optimization of the enzymatic elimination of flumequine by laccase-mediated system using response surface methodology, Desalin. Water Treat. (2015) 1–10.
[47] S. Ashrafi, H. Kamani, A. Mahvi, The optimization study of direct red 81 and methylene blue adsorption on NaOH-modified rice husk, Desalin. Water Treat. (2014) 1–9.
[48] M. Samarghandi, M. Zarrabi, M. Sepehr, A. Amrane, G. Safari, S. Bashiri, Application of acidic treated pumice as an adsorbent for the removal of azo dye from aqueous solutions: Kinetic, equilibrium and thermodynamic studies, Iran. J. Environ. Health Sci. Eng. 9 (2011) 9–19.
[49] R.S. Wu, K.H. Lam, J. Lee, T. Lau, Removal of phosphate from water by a highly selective La(III)-chelex resin, Chemosphere 69 (2007) 289–294.
[50] G.H. Safari, S. Bashiri, Application of acidic treated pumice as an adsorbent for the removal of azo dye from aqueous solutions: Kinetic, equilibrium and thermodynamic studies, Iran. J. Environ. Health Sci. Eng. 9 (2012) 1–9.
[51] M. Samadi, M. Saghi, K. Ghadiri, M. Hadi, M. Beikmohammadi, Performance of simple nano zeolite Y and modified nano zeolite Y in phosphor removal from aqueous solutions, Iran. J. Health Environ. 3 (2010) 27–36.
[52] M.R. Boldaji, A. Mahvi, S. Dobaradaran, S. Hosseini, Evaluating the effectiveness of a hybrid sorbent resin in removing fluoride from water, Int. J. Environ. Sci. Technol. 6 (2009) 629–632.
[53] W. Huang, S. Wang, Z. Zhu, L. Li, X. Yao, V. Rudolph, F. Haghseresht, Phosphate removal from wastewater using red mud, J. Hazard. Mater. 158 (2008) 35–42.

[54] M. Dundar, C. Nuhoglu, Y. Nuhoglu, Biosorption of Cu(II) ions onto the litter of natural trembling poplar forest, J. Hazard. Mater. 151 (2008) 86–95.
[55] U.R. Malik, S.M. Hasany, M.S. Subhani, Sorptive potential of sunflower stem for Cr(III) ions from aqueous solutions and its kinetic and thermodynamic profile, Talanta 66 (2005) 166–173.
[56] C. Namasivayam, D. Sangeetha, Equilibrium and kinetic studies of adsorption of phosphate onto $ZnCl_2$ activated coir pith carbon, J. Colloid Interface Sci. 280 (2004) 359–365.
[57] M. Özacar, Equilibrium and kinetic modelling of adsorption of phosphorus on calcined alunite, Adsorption 9 (2003) 125–132.
[58] S.-X. Li, Z. Feng-Ying, H. Yang, N. Jian-Cong, Thorough removal of inorganic and organic mercury from aqueous solutions by adsorption on *Lemna minor* powder, J. Hazard. Mater. 186 (2011) 423–429.